
DOGE-Train: Discrete Optimization on GPU with End-to-end Training

Ahmed Abbas

MPI for Informatics
Saarland Informatics Campus

Paul Swoboda

Abstract

We present a fast, scalable, data-driven approach for solving linear relaxations of 0-1 integer linear programs using a graph neural network. Our solver is based on the Lagrange decomposition based algorithm [1]. We make the algorithm differentiable and perform backpropagation through the dual update scheme for end-to-end training of its algorithmic parameters. This allows to preserve the algorithm’s theoretical properties including feasibility and guaranteed non-decrease in the lower bound. Since [1] can get stuck in suboptimal fixed points, we provide additional freedom to our graph neural network to predict non-parametric update steps for escaping such points while maintaining dual feasibility. For training of the graph neural network we use an unsupervised loss and perform experiments on large-scale real world datasets. We train on smaller problems and test on larger ones showing strong generalization performance with a graph neural network comprising only around 10^k parameters. Our solver achieves significantly faster performance and better dual objectives than its non-learned version [1]. In comparison to commercial solvers our learned solver achieves close to optimal objective values of LP relaxations and is faster by up to an order of magnitude on very large problems from structured prediction and on selected combinatorial optimization problems. Our code will be made available upon acceptance.

1 Introduction

Integer linear programs (ILP) are a universal tool for solving combinatorial optimization problems. While great progress has been made on improving ILP solvers over the past several decades, some fundamental questions for future improvements remain open: Can ILP solvers make effective use of the massive parallelism afforded by GPUs and can modern machine learning meaningfully help? As of now the consensus seems that neither GPUs nor ML have yet helped general purpose ILP solvers in a fundamental way. In particular, this holds true for LP solvers which are a key component of most commonly used ILP approaches. LP solvers produce lower bounds on the optimal solution objective and are integral for many heuristics to decode feasible integral solutions. For many problems the ILP solvers spend most of the time on solving multiple LP relaxations, hence any impact GPUs and ML can have will directly translate into overall improvement of ILP solvers.

State of the art LP solvers [23, 13, 17, 4, 18] make little utility of modern machine learning but rather use either hand-designed or auto-tuned parameters and update rules. Moreover, with the exception of [18] these solvers are not open-source, hence researchers’ ability to assess the potential of neural networks for improving LP solvers is limited. From a conceptual point of view traditional solver paradigms, e.g. simplex or interior point methods, are not GPU friendly and contain non-differentiable steps (such as pivot selection for simplex). Additionally, their high complexity further complicates any effort at making them differentiable. This makes utilization of neural networks and GPUs for solver improvement difficult.

We propose a new way to use the potential of GPU parallelism and modern ML to obtain advances in LP relaxation solvers for ILPs. We argue that due to the difficulties in putting GPUs and ML to work in traditional solver methodologies, investigation of new paradigms is called for. To this end we build upon the recent work of [1] which proposed a massively parallel GPU friendly solver for 0-1 integer linear programming using Lagrange decomposition. The solver exhibits faster performance than traditional CPU solvers on large-scale problems making good use of GPU parallelism. Also due to its comparatively simple control flow and its usage of simple arithmetic operations for all its operations it can be made differentiable. This allows to train its parameters and predict update steps that will allow for faster convergence and overcoming fixed points from which the basic version of the algorithm suffers. This results in superior performance as compared to the non-learned version [1]. We obtain small gaps to (D)LP optima on a diverse range of large scale structured prediction problems, QAPLib [8] and independent set problems [39]. We are up to an order of magnitude faster than traditional ILP solvers.

Contributions We propose to learn the Lagrange decomposition based algorithm [1] for solving LP relaxations of ILP problems and show its benefits. In particular,

- We make the dual update steps of [1] differentiable. This allows us to predict parameters of the update steps so that faster convergence is achieved as compared to using hand-picked values.
- We train a predictor for arbitrary non-parametric update steps that allow to escape suboptimal fixed points into which the parametric update steps of [1] can fall.
- We propose to train predictors for both the parametric and non-parametric updates in fully unsupervised manner. Our loss optimizes for parameters/update steps producing large improvements in the dual lower bound over a long time horizon.
- We show the benefits of our learned massively parallel GPU approach on a wide range of problems. We have chosen structured prediction tasks including graph matching [29] and cell tracking [24]. From theoretical computer science we compare on the QAPLib [8] dataset and randomly generated independent set problems [39].

2 Related Work

2.1 Learning to solve Combinatorial Optimization

ML has been used to improve various aspects of solving combinatorial problems. For the standard branch-and-cut ILP solvers the works [19, 22, 35] learn variable selection for branching. The approaches [14, 35] learn to fix a subset of integer variables in ILPs to their hopefully optimal values to improve finding high quality primal solutions. The works [43, 54] learn variable selection for the large neighborhood search heuristic for obtaining primal solutions to ILPs. Selecting good cuts through scoring them with neural networks was investigated in [26, 46]. While all these approaches result in runtime and solution quality improvements, only a few works tackle the important task of speeding up ILP relaxations by ML. Specifically, the work [11] used graph neural network (GNN) to predict variable orderings of decision diagrams representing combinatorial optimization problems. The goal is to obtain an ordering such that a corresponding dual lower bound is maximal. To our knowledge it is the only work that addresses computing ILP relaxations with ML. For constraint satisfaction problems [40, 9, 47] train GNN while [47] train in an unsupervised manner. For narrow subclasses of problems primal heuristics have been augmented through learning some of their decisions, e.g. for capacitated vehicle routing [36] and traveling salesman [55]. For a more complete overview of ML for combinatorial optimization we refer to the detailed surveys [6, 10].

2.2 Massively parallel combinatorial optimization

Massively parallel algorithms running on GPU have been proposed for narrow problem classes, including inference in [41, 56] and dense [45] Markov Random Fields, multicut [2] and for max-flow [49, 53]. The algorithm [1] on which our work is based is, to our knowledge, the only generic ILP solver that can make adequate use of parallelism offered by GPUs.

2.3 Unrolling algorithms for parameter learning

Algorithms containing differentiable iterative procedures are combined with neural networks for improving performance of such algorithms. One of the earliest works in this direction is [21] which embedded sparse coding algorithms in a neural network by unrolling. For solving inverse problems [57, 12] unroll through ADMM and non-linear diffusion resp. Overall, such approaches show more generalization power than pure neural networks based ones as shown in the survey [34]. Slightly different than from the above works, neural networks were used to predict update directions for training other neural networks (e.g. in [3]).

3 Method

We first recapitulate the Lagrange decomposition approach to binary ILPs from [31] and the deferred min-marginal averaging scheme for its solution proposed in [1]. We highlight possible parameters of the update steps which we will predict by training a graph neural network. Proofs are in the Appendix.

3.1 Lagrange Decomposition & Deferred Min-Marginal Averaging

Definition 1 (Binary Program [31]). Let a linear objective $c \in \mathbb{R}^n$ and m variable subsets $\mathcal{I}_j \subset [n]$ of constraints with feasible set $\mathcal{X}_j \subset \{0, 1\}^{\mathcal{I}_j}$ for $j \in [m]$ be given. The corresponding binary program is

$$\min_{x \in \{0, 1\}^n} \langle c, x \rangle \quad \text{s.t.} \quad x_{\mathcal{I}_j} \in \mathcal{X}_j \quad \forall j \in [m], \quad (\text{BP})$$

where $x_{\mathcal{I}_j}$ is the restriction to variables in \mathcal{I}_j .

Any binary ILP $\min_{x \in \{0, 1\}^n} \langle c, x \rangle$ s.t. $Ax \leq b$ where $A \in \mathbb{R}^{m \times n}$ can be written as (BP) by associating each constraint $a_j^T x \leq b_j$ for $j \in [m]$ with its own subproblem \mathcal{X}_j .

In order to obtain a problem formulation amenable for parallel optimization we consider its Lagrange dual which decomposes the full problem (BP) into a series of coupled subproblems.

Definition 2 (Lagrangian dual problem [31]). Define the set of subproblems that constrain variable i as $\mathcal{J}_i = \{j \in [m] \mid i \in \mathcal{I}_j\}$. Let the energy for subproblem $j \in [m]$ w.r.t. Lagrangian dual variables $\lambda_{\bullet, j} = (\lambda_{ij})_{i \in \mathcal{I}_j} \in \mathbb{R}^{\mathcal{I}_j}$ be

$$E^j(\lambda_{\bullet, j}) = \min_{x \in \mathcal{X}_j} \langle \lambda_{\bullet, j}, x \rangle. \quad (1)$$

Then the Lagrangian dual problem is defined as

$$\max_{\lambda} \sum_{j \in [m]} E^j(\lambda_{\bullet, j}) \quad \text{s.t.} \quad \sum_{j \in \mathcal{J}_i} \lambda_{ij} = c_i \quad \forall i \in [n]. \quad (\text{D})$$

The authors in [1] have proposed a parallelization friendly iterative algorithm for updating Lagrange multipliers λ for maximizing (D), see Algorithm 1. We write it in a slightly adapted form since it will allow us to easily describe its backpropagation. The algorithm assigns the Lagrange variables in u -many disjoint blocks B_1, \dots, B_u in such a way that each block contains at most one Lagrange variable from each subproblem and all variables within a block are updated in parallel. The dual update scheme relies on computing min-marginal differences i.e., the difference of subproblem objectives when a certain variable is set to 1 minus its objective when the same variable is set to 0, see line 10 in Algorithm 1. These min-marginal differences are averaged out across subproblems via updates to Lagrange variables in line 11 in Algorithm 1. The crucial ingredient allowing parallelization is that in the min-marginal averaging step values from the last iteration are used (i.e. M^{in}), making synchronization between subproblems unnecessary.

In [1] the min-marginal averaging parameters of Algorithm 1 were set as $\omega = 0.5$ and $\alpha_{ij} = 1/|\mathcal{J}_i|$ leading to uniform averaging. We generalize the min-marginal update step by considering more general parametric update steps. We allow $\omega \in (0, 1)$ and α -values to be arbitrary convex combinations. In the next section we will show how to train these values to achieve faster convergence.

Proposition 1 (Dual Feasibility and Monotonicity of Min-marginal Averaging). *For any $\alpha_{ij} \geq 0$ with $\sum_{j \in \mathcal{J}_i} \alpha_{ij} = 1$ and $\omega_{ij} \in [0, 1]$ the min-marginal averaging step in line 11 in Algorithm 1 retains dual feasibility and is non-decreasing in the dual lower bound.*

Algorithm 1: Parallel Deferred Min-Marginal Averaging [1]

Input: Lagrange variables $\lambda_{ij} \forall i \in [n], j \in \mathcal{J}_i$, damping factors $\omega_{ij} \in (0, 1) \forall i \in [n], j \in \mathcal{J}_i$, anisotropic min-marginal averaging weights $\alpha_{ij} \in (0, 1) \forall i \in [n], j \in \mathcal{J}_i$, max. number of iterations T .

- 1 Initialize deferred min-marginal diff. $M = 0$
- 2 **for** T iterations **do**
- 3 **for** block $B \in (B_1, \dots, B_u)$ **do**
- 4 $\lambda, M \leftarrow \text{BlockUpdate}(B, \lambda, M, \alpha, \omega)$
- 5 **for** block $B \in (B_u, \dots, B_1)$ **do**
- 6 $\lambda, M \leftarrow \text{BlockUpdate}(B, \lambda, M, \alpha, \omega)$
- 7 **return** λ, M
- 8 **Procedure** $\text{BlockUpdate}(B, \lambda^{\text{in}}, M^{\text{in}}, \alpha, \omega)$
- 9 **for** $ij \in B$ in parallel **do**
- 10 Compute $M_{ij}^{\text{out}} = \omega_{ij} [\min_{x \in \mathcal{X}_j: x_i=1} \langle \lambda_{\bullet j}^{\text{in}}, x \rangle - \min_{x \in \mathcal{X}_j: x_i=0} \langle \lambda_{\bullet j}^{\text{in}}, x \rangle]$
- 11 Update $\lambda_{ij}^{\text{out}} = \lambda_{ij}^{\text{in}} - M_{ij}^{\text{out}} + \alpha_{ij} \sum_{k \in \mathcal{J}_i} M_{ik}^{\text{in}}$
- 12 **return** $\lambda^{\text{out}}, M^{\text{out}}$

3.2 Backpropagation through Deferred Min-Marginal Averaging

We show below how to differentiate through Algorithm 1 with respect to the parameters α and ω . This will ultimately allow us to learn these parameters such that faster convergence is achieved. To this end we describe backpropagation for a block update (lines 8- 12) of Alg. 1. All other operations can be tackled by automatic differentiation. For a block B in $\{B_1, \dots, B_u\}$ we view the Lagrangean update as a mapping $\mathcal{H} : (\mathbb{R}^{|B|})^4 \rightarrow (\mathbb{R}^{|B|})^2, (\lambda^{\text{in}}, M^{\text{in}}, \alpha, \omega) \mapsto (\lambda^{\text{out}}, M^{\text{out}})$.

Given a loss function $\mathcal{L} : \mathbb{R}^N \rightarrow \mathbb{R}$ we denote $\partial \mathcal{L} / \partial x$ by \dot{x} . Algorithm 2 shows backpropagation through \mathcal{H} to compute the gradients $\dot{\lambda}^{\text{in}}, \dot{M}^{\text{in}}, \dot{\alpha}$ and $\dot{\omega}$.

Proposition 2. *Algorithm 2 performs backpropagation through \mathcal{H} .*

Efficient Implementation Generally, the naive computation of min-marginal differences and its backpropagation are both expensive operations as they require solving two optimization problems for each dual variable. In [1, 31] the authors represented each subproblem using binary decision diagrams (BDDs) for fast incremental computation of min-marginal differences. Their algorithm results in a computation graph involving only elementary arithmetic operations and taking minima over several variables. Using this computational graph we can implement the abstract Algorithm 2 efficiently and parallelize on GPU. For details we refer to the Appendix.

Algorithm 2: BlockUpdate backpropagation

Input: Forward pass inputs: $B, \lambda^{\text{in}}, M^{\text{in}}, \alpha, \omega$, gradients of forward pass output: $\dot{\lambda}^{\text{out}}, \dot{M}^{\text{out}}$, gradients of parameters $\dot{\alpha}, \dot{\omega}$

- 1 **for** $ij \in B$ in parallel **do**
- 2 $\dot{M}_{ij}^{\text{in}} = \sum_{k \in \mathcal{J}_i} \dot{\lambda}_{ik}^{\text{out}} \alpha_{ik}, \quad \dot{M}_{ij}^{\text{out}} = \dot{M}_{ij}^{\text{out}} - \dot{\lambda}_{ij}^{\text{out}}$
- 3 $\dot{\alpha}_{ij} = \dot{\alpha}_{ij} + \dot{\lambda}_{ij} \sum_{k \in \mathcal{J}_i} M_{ik}^{\text{in}}, \quad \dot{\omega}_{ij} = \dot{\omega}_{ij} + M_{ij}^{\text{out}} [M_{ij}^{\text{out}} / \omega_{ij}]$
- 4 Compute minimizers $s^j(i, \beta) = \arg \min_{x \in \mathcal{X}_j: x_i=\beta} \langle \lambda_{\bullet j}^{\text{in}}, x \rangle, \forall \beta \in \{0, 1\}$
- 5 $\dot{\lambda}_{pj}^{\text{in}} = \dot{\lambda}_{pj}^{\text{out}} + M_{ij}^{\text{out}} \omega_{ij} [s_p^j(i, 1) - s_p^j(i, 0)], \forall p \in \mathcal{I}_j$
- 6 **return** $\dot{\lambda}^{\text{in}}, \dot{M}^{\text{in}}, \dot{\alpha}, \dot{\omega}$

3.3 Non-Parametric Update Steps

Although the min-marginal averaging scheme of Alg. 1 guarantees non-decreasing lower bound, it can get stuck in suboptimal fixed points, see [50] for a discussion for the special case of MAP-MRF. To alleviate this shortcoming we allow arbitrary updates to Lagrange variables through a vector

$\theta \in \mathbb{R}^{|\lambda|}$ as

$$\lambda_{ij} \leftarrow \lambda_{ij} + \theta_{ij} - \frac{1}{|\mathcal{J}_i|} \sum_{k \in \mathcal{J}_i} \theta_{ik}, \forall i \in [n], j \in \mathcal{J}_i \quad (2)$$

where the last term ensures feasibility of updated Lagrange variables w.r.t. the dual problem (D).

3.4 Graph neural network

We train a graph neural network (GNN) to predict the parameters α, ω of Alg. 1 and also the non-parametric update θ for (2). To this end we encode the dual problem (D) on a bipartite graph $\mathcal{G} = (\mathcal{V}, \mathcal{E})$. Its nodes correspond to primal variables \mathcal{I} and subproblems \mathcal{J} i.e., $\mathcal{V} = \mathcal{I} \cup \mathcal{J}$ and edges $\mathcal{E} = \{ij \mid i \in \mathcal{I}, j \in \mathcal{J}_i\}$ correspond to Lagrange multipliers. We need to predict values of α_{ij}, ω_{ij} and θ_{ij} for each edge ij in \mathcal{E} . We associate features $f = (f_{\mathcal{I}}, f_{\mathcal{J}}, f_{\mathcal{E}})$ with each entity of the graph which capture the current state of Alg. 1. Additionally, we encode a number of quantities as features which can make learning easier. For example, a history of previous dual objectives for each subproblem is encoded in the constraint nodes and minimizers of each subproblem (which correspond to a subgradient of the dual problem (D)) are encoded in the edge features $f_{\mathcal{E}}$. A complete list of features is provided in the Appendix.

Message passing To perform message passing we use the transformer based graph convolution scheme of [42]. We first compute an embedding of all subproblems j in \mathcal{J} by receiving messages from adjacent nodes and edges as

$$\text{CONV}_{\mathcal{J}}(f_{\mathcal{I}}, f_{\mathcal{J}}, f_{\mathcal{E}}, \mathcal{E})_j = \mathbf{W}_s f_j + \sum_{i|ij \in \mathcal{E}} a_{ij}(f_j, f_{\mathcal{I}}, f_{\mathcal{E}}; \mathbf{W}_a) [\mathbf{W}_t f_i + \mathbf{W}_e f_{ij}], \quad (3)$$

where $\mathbf{W} = (\mathbf{W}_a, \mathbf{W}_s, \mathbf{W}_t, \mathbf{W}_e)$ are trainable parameters and $a_{ij}(f_j, f_{\mathcal{I}}, f_{\mathcal{E}}; \mathbf{W}_a)$ is the softmax attention weight between nodes i and j parameterized by \mathbf{W}_a . Afterwards we perform message passing in the reverse direction to compute embeddings for primal variables \mathcal{I} . Similar strategy for message passing on a bipartite graph was followed by [19].

Recurrent connections Our default GNN as mentioned above only uses hand-crafted features to maintain a history of previous optimization rounds. To learn a summary of the past updates we optionally allow recurrent connections through an LSTM with forget gate [20]. The LSTM is only applied on primal variable nodes \mathcal{I} and maintains cell states $s_{\mathcal{I}}$ which can be updated and used for parameter prediction in subsequent optimization rounds.

Prediction The learned embeddings from GNN, LSTM outputs and solver features from Alg. 1 are consumed by a multi-layer perceptron Φ to predict the required variables for each edge ij in \mathcal{E} . Afterwards we transform these outputs so that they satisfy Prop. 1.

The exact sequence of operations performed by the graph neural network are shown in Alg. 3 where $[u_1, \dots, u_k]$ denotes concatenation of vectors u_1, \dots, u_k , LN denotes layer normalization [5] and $\text{LSTM}_{\mathcal{I}}$ stands for an LSTM cell which operates on each primal variable node.

Algorithm 3: Parameter prediction by GNN

Input: Primal variable features $f_{\mathcal{I}}$ and cell states $s_{\mathcal{I}}$, Subproblem features $f_{\mathcal{J}}$, Dual variable (edge) features $f_{\mathcal{E}}$, Set of edges \mathcal{E} .

- 1 $h_{\mathcal{J}} = \text{ReLU}(\text{LN}(\text{CONV}_{\mathcal{J}}(f_{\mathcal{I}}, f_{\mathcal{J}}, f_{\mathcal{E}}, \mathcal{E})))$ // Compute subproblems embeddings
 - 2 $h_{\mathcal{I}} = \text{ReLU}(\text{LN}(\text{CONV}_{\mathcal{I}}(f_{\mathcal{I}}, [f_{\mathcal{J}}, h_{\mathcal{J}}], f_{\mathcal{E}}, \mathcal{E})))$ // Compute primal variable embeddings
 - 3 $z_{\mathcal{I}}, s_{\mathcal{I}} = \text{LSTM}_{\mathcal{I}}(h_{\mathcal{I}}, s_{\mathcal{I}})$ // Compute output and cell state
 - 4 $(\hat{\alpha}, \hat{\omega}, \theta) = \Phi([f_{\mathcal{I}}, h_{\mathcal{I}}, z_{\mathcal{I}}], [f_{\mathcal{J}}, h_{\mathcal{J}}], f_{\mathcal{E}}, \mathcal{E})$ // Prediction per edge
 - 5 $\alpha_{i\bullet} = \text{Softmax}(\hat{\alpha}_{i\bullet}), \forall i \in \mathcal{I}, \omega = \text{Sigmoid}(\hat{\omega})$ // Ensure non-decreasing obj., Prop. 1
 - 6 **return** $\alpha, \omega, \theta, s_{\mathcal{I}}$
-

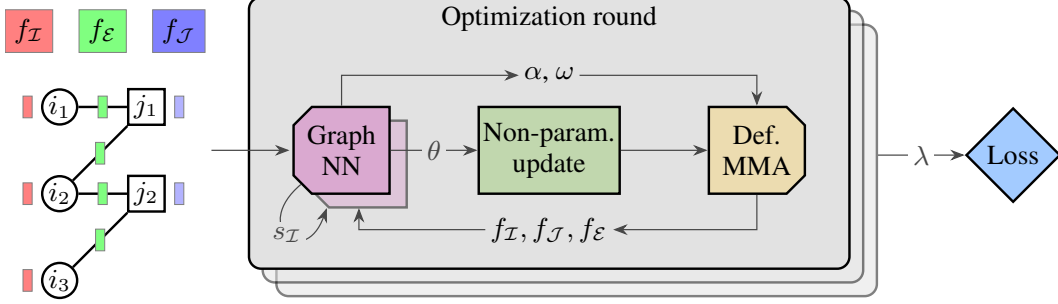


Figure 1: Our pipeline for optimizing the Lagrangean dual (D). The problem is encoded on a bipartite graph containing features $f_{\mathcal{I}}$, $f_{\mathcal{J}}$ and $f_{\mathcal{E}}$ for primal variables, subproblems and dual variables resp. A graph neural network (GNN) predicts the non-parameteric update θ (2) and parameters α and ω for Alg. 1. In one optimization round current set of Lagrange multipliers λ are first updated by the non-parametric update using θ . Afterwards deferred min-marginal averaging is performed parameterized by α and ω . The updated solver features f (which also includes λ) and LSTM cell states $s_{\mathcal{I}}$ are sent to the GNN in next optimization round. These rounds are repeated at most R -times during training and until convergence during inference.

3.5 Loss

Given the Lagrange variables λ we directly use the dual objective (D) as an unsupervised loss to train the GNN. Thus, we maximize the loss L defined as

$$\mathcal{L}(\lambda) = \sum_{j \in [m]} E^j(\lambda_{\bullet j}). \quad (4)$$

For a mini-batch of instances during training we take the mean of corresponding per-instance losses. For backpropagation, gradient of loss \mathcal{L} w.r.t. Lagrange variables of a subproblem j is computed by finding a minimizing assignment for that subproblem, written as

$$\left(\frac{\partial \mathcal{L}}{\partial \lambda} \right)_{\bullet j} = \operatorname{argmin}_{x \in \mathcal{X}_j} \langle \lambda_{\bullet j}, x \rangle \in \{0, 1\}^{\mathcal{I}_j}. \quad (5)$$

The above gradient is then sent as input for backpropagation. For computing the minimizing assignment efficiently we use binary decision diagram representation of each subproblem as in [1, 31].

3.6 Overall pipeline

Our overall pipeline combining all building blocks from the previous sections is shown in Figure 1. We train our pipeline which contains multiple dual optimization rounds in a fashion similar to that of recurrent neural networks. One round of our dual optimization consists of message passing by GNN, a non-parametric update step and T iterations of deferred min-marginal averaging. For computational efficiency we run our pipeline for at most R dual optimization rounds during training. On each mini-batch we randomly sample a number of optimization rounds r in $[R]$, run $r - 1$ rounds without tracking gradients and backpropagate through the last round by computing the loss (4). For the pipeline with recurrent connections we backpropagate through last 3 rounds and apply the loss after each of these rounds. Since the task of dual optimization is relatively easier in early rounds as compared to later ones (where [1] can get stuck) we use two neural networks. The early stage network is trained if the randomly sampled r is in $[0, R/2]$ and the late stage network is chosen otherwise. During testing we switch to the later stage network when the relative improvement in the dual objective by the early stage network becomes less than 10^{-6} .

4 Experiments

As main evaluation metric we report convergence plots of the relative dual gap $g(t) \in [0, 1]$ at time t

$$g(t) = \min \left(\frac{d^* - d(t)}{d^* - d_{init}}, 1.0 \right) \quad (6)$$

where $d(t)$ is the dual objective at time t , d^* is the optimal (or best known) objective value of the Lagrange relaxation (D) and d_{init} is the objective value before optimization as computed by [1]. Additionally we also report per dataset averages of relative dual gap integral $g_I = \int g(t)dt$ [7], best objective value (E) and time taken (t) to obtain best objective. To cater the dominating effect of worse initial lower bounds on g_I (as $g(t)$ can be close to 1 at $t \approx 0$) we start calculating g_I after a few rounds of our solver are completed. This start time is then also used to evaluate other algorithms for a fair comparison. To evaluate CPU solvers we use an AMD EPYC 7702 CPU. For the GPU solvers we use either one NVIDIA RTX 8000 (48GB) or A100 (80GB) GPU depending on instance size.

4.1 Algorithms

Gurobi: Results of the dual simplex algorithm from the commercial ILP solver [23].

FastDOG: The non-learned baseline [1] of Alg. 1 with $\omega_{ij} = 0.5$ and $\alpha_{ij} = 1/|\mathcal{J}_i|$.

DOGE: Our approach where we learn to predict parametric and non-parametric updates by using two graph neural networks for early and late-stage optimization. Size of the learned embeddings h computed by the GNN in Alg. 3 is set to 16 for nodes and 8 for edges. For computing attention weights in (3) we use only one attention head for efficiency. The predictor Φ in Alg. 3 contains 4 linear layers with the ReLU activation. We train the networks using the Adam optimizer [30]. To prevent gradient overflow we use gradient clipping on model parameters by an l^2 norm of 50. The number of trainable parameters is $8k$.

DOGE-M: Variant of our method where we additionally use recurrent connections using LSTM. The cell state vector s_i for each primal variable node $i \in \mathcal{I}$ has a size of 16. The number of trainable parameters is $12k$.

We have not tested against specialized heuristics for our benchmark problems since [1] has shown them to be on par or outperformed by FastDOG. For training our approach we use the frameworks [15, 16, 38] and implement the Algorithms 1,2 in CUDA [37] using [25, 28].

4.2 Datasets

Cell tracking (CT): Instances of developing flywing tissue from cell tracking challenge [48] processed by [24] and obtained from [44]. We use the largest and hardest 3 instances, train on the 2 smaller instances and test on the largest one.

Graph matching (GM): Instances of graph matching for matching nuclei in 3D microscopic images [32] processed by [29] and made publicly available through [44]. We train on 10 instances and test on the remaining 20 instances.

Independent set (IS): Random instances of independent set problem generated using [39]. For training we generate 240 instances with $10k$ vertices each and test on 60 instances with $50k$ vertices. We generating edges between vertices in the graph with a probability of 0.25.

QAPLib: The benchmark dataset for quadratic assignment problems used in the combinatorial optimization community [8]. We train on 61 instances having up to 40 nodes and test on 35 instances having up to 70 nodes.

For each dataset we use a separate set of hyperparameters due to varying instance sizes given in Table 1. All our test datasets on average contain more than a million edges (i.e., Lagrange variables) while training instances are considerably smaller. For efficiency, during evaluation we use a larger value of T in Alg. 1 than during training. For the *CT* dataset containing we learn only the non-parametric update steps (2) and fix the parameters in Alg. 1 to their default values from [1]. Learning these parameters gave slightly worse training loss at convergence.

4.3 Ablation study

We perform an ablation study to test the importance of various components of our approach. Starting from [1] as a baseline we first predict all parameters α, ω, θ through the two multi-layer perceptrons Φ for early and late stage optimization without using GNN. Next, we report results of using one network (instead of two) which is trained and tested for both early and later rounds of dual optimization. Lastly, we aim to seek the importance of learning parameters of Alg. 2 and the non-parametric update (2). To this end, we learn to predict only the non-parametric update and apply the loss directly on updated

Table 1: Hyperparameters of our approach and dataset statistics. $|\mathcal{I}| + |\mathcal{J}|$: Average number of variables and constraints in each dataset (# vertices in GNN); $\sum_{j=1}^m |\mathcal{J}_j|$: Average number of Lagrange multipliers (# edges in GNN); T : Number of iterations of Alg. 1 in each optimization round; R : max. number of training rounds; # itr. train: Number of training iterations.

Dataset	$ \mathcal{I} + \mathcal{J} (\times 10^6)$		$\sum_{j=1}^n \mathcal{J}_j (\times 10^6)$		T		R	batch size	learn. rate	# itr. train	train time [hrs]
	train	test	train	test	train	test					
<i>CT</i>	3.7	12.4	8.5	28	1	100	400	1	1e-3	500	14
<i>GM</i>	1.7	1.7	3.3	3.3	20	200	20	2	1e-3	400	4
<i>IS</i>	0.05	0.4	0.1	1.2	20	50	20	8	1e-3	2500	10
<i>QAPLib</i>	0.1	2.8	0.5	11	5	20	500	4	1e-3	1600	48

Table 2: Ablation study results on the *Graph matching* dataset. w/o GNN: Use only the two predictors Φ without GNN for early and late stage optimization; same network: use one network (GNN, Φ) for both early and late stage; only non-param., param.: predict only the non-parametric update (2) or the parametric update (Alg. 1); w/o α , ω : does not predict α or ω resp.

	w/o learn. (1)	w/o GNN	same network	only non-param.	only param.	w/o α	w/o ω	DOGE	DOGE-M
g_I (\downarrow)	21	0.42	0.95	2.3	0.7	0.36	0.35	0.33	0.19
E (\uparrow)	-48912	-48440	-48444	-48476	-48444	-48439	-48439	-48439	-48436
$t[s]$ (\downarrow)	61	29	24	51	74	30	30	17	21

λ without requiring backpropagation through Alg. 1. We also try learning a subset of parameters i.e., not predicting averaging weights α or damping factors ω . Lastly, we report results of DOGE-M which uses recurrent connections. The results are in Table 2.

Firstly, from our ablation study we observe that learning even one of the two types of updates i.e., non-parametric or parametric already gives better results than the non-learned solver [1]. This is because non-parametric update can help in escaping fixed-points of [1] when they occur and the parametric update can help Alg. 1 in avoiding such fixed-points. Combining both of these strategies further improves the results. Secondly, we observe that performing message passing with GNN gives improvement over only using the predictor Φ . Thirdly, we find using separate networks for early and late stage optimization gives better performance than using the same network for all stages. Lastly, using recurrent connections gives the best performance.

4.4 Results

Convergence plots of relative dual gaps change w.r.t. wall clock times are given in Figure 2. Rest of the evaluation metrics are reported in Table 3. For further details we refer to the Appendix.

Discussion As compared to the non-learned baseline FastDOG we reach an order of magnitude more accurate relaxation solutions, almost closing the gap to optimum as computed by Gurobi. We retain high speed afforded by exploiting GPU parallelism. Interestingly, we can often outperform FastDOG also in the early stage where optimization is easy. Our LSTM version DOGE-M has shown improved performance than the non-LSTM version. Especially it shows much improvement on the most difficult *QAPLib* dataset. On *QAPLib* Gurobi does not converge on instances with more than

Table 3: Results comparison on all datasets where the values are averaged within a dataset. Numbers in bold highlight the best performance.

	<i>Cell tracking</i>			<i>Graph matching</i>			<i>Independent set</i>			<i>QAPLib</i>		
	g_I	$E(\times 10^8)$	$t[s]$	g_I	$E(\times 10^4)$	$t[s]$	g_I	$E(\times 10^8)$	$t[s]$	g_I	$E(\times 10^6)$	$t[s]$
Gurobi [23]	18	-3.852	809	9	-4.8433	278	14	-2.4457	52	3472	0.9	2618
FastDOG [1]	7	-3.863	1005	21	-4.8912	61	42	-2.4913	9	276	5.7	1680
DOGE	2.4	-3.854	1015	0.3	-4.8439	17	0.3	-2.4460	8	320	12.1	720
DOGE-M	2.1	-3.854	730	0.2	-4.8436	21	0.2	-2.4459	5	131	14.5	861

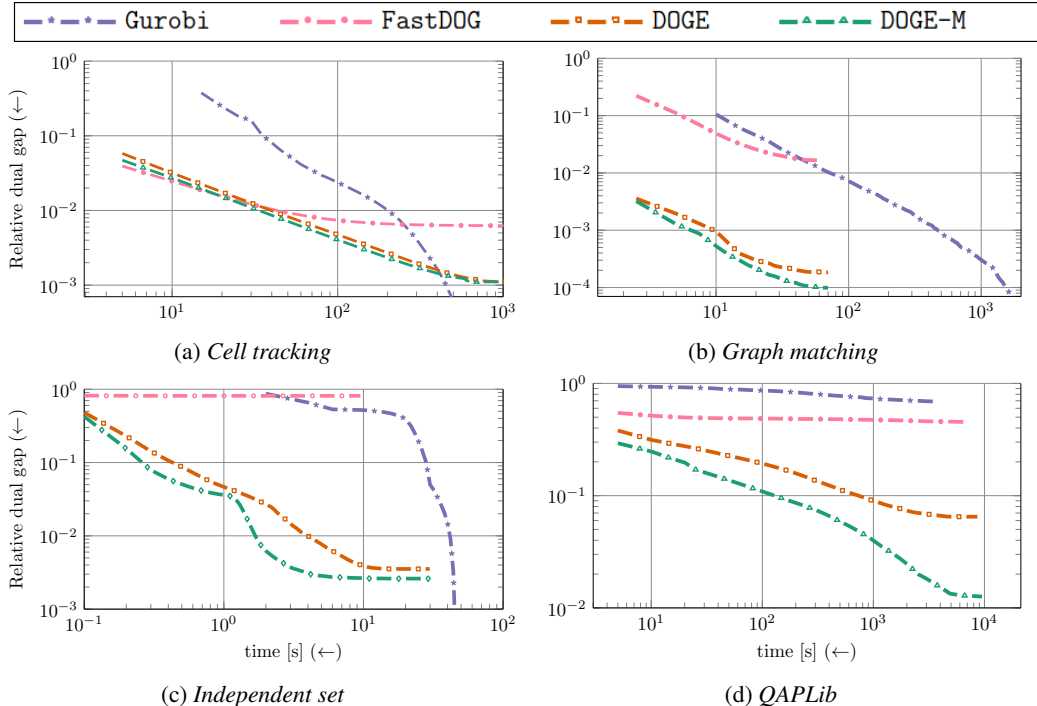


Figure 2: Convergence plots for $g(t)$ defined in (6), the relative dual gap to the optimum (or maximum suboptimal objective among all methods) of the relaxation (D). Both axes are logarithmic.

40 nodes within the time limit of one hour. We show convergence plots for smaller instances in the Appendix. The difference to Gurobi is most pronounced w.r.t. anytime performance measured by g_I , since our solver reaches good solutions relatively early.

Limitations While our approach gives solutions of high accuracy for the presented datasets, we have also tried our approach on other datasets (small cell tracking instances, MRFs for protein folding [27] and shape matching [51, 52]) where we were not able to obtain significant improvements w.r.t. the non-learned baseline [1]. For small cell tracking instances FastDOG already found the optimum in a moderate number of iterations, making it hard to beat. On shape matching and protein folding the parallelization of FastDOG did not bring enough speed-ups due to few large subproblems resulting in sequential bottlenecks. This limited the number of training iterations we could perform within a reasonable time.

We have set some hyperparameters in a dataset-dependent way. This was partly necessitated due to problem sizes e.g., training on long time horizons was not possible with very large instances. Moreover, these instances only permitted a limited number of parameters in our neural networks.

5 Conclusion

We have proposed a learning approach for solving relaxations to combinatorial optimization problems by backpropagating through and learning parameters for the non-learned baseline [1]. We demonstrated its potential in obtaining close to optimal solutions faster than with traditional methods.

Our work raises interesting follow-up questions: (i) Contrary to many approaches for backpropagation which replace non-smooth operations with smoothed variants (e.g. [33]) we directly compute (sub-)gradients for the non-smooth solver updates. Can smoothing of the solver help obtain a better backpropagated supervision? (ii) We argue that predicting good update steps for our solver is in itself an interesting and challenging problem for GNNs. We hope that our work can become a testbed for GNN architectures. (iii) There are a few desiderata for future learned solvers, including training universal models that generalize across different problem classes. Possibly more powerful GNNs and more involved training regimes are needed for this.

References

- [1] Ahmed Abbas and Paul Swoboda. FastDOG: Fast discrete optimization on GPU. In *Proceedings of the IEEE Conference on Computer Vision and Pattern Recognition*, 2022. (Cited on p. 1, 2, 3, 4, 6, 7, 8, 9, 13, 15)
- [2] Ahmed Abbas and Paul Swoboda. RAMA: A Rapid Multicut Algorithm on GPU. In *Proceedings of the IEEE Conference on Computer Vision and Pattern Recognition*, 2022. (Cited on p. 2)
- [3] Marcin Andrychowicz, Misha Denil, Sergio Gomez, Matthew W Hoffman, David Pfau, Tom Schaul, Brendan Shillingford, and Nando De Freitas. Learning to learn by gradient descent by gradient descent. *Advances in neural information processing systems*, 29, 2016. (Cited on p. 3)
- [4] MOSEK ApS. *9.0.105*, 2022. (Cited on p. 1)
- [5] Jimmy Lei Ba, Jamie Ryan Kiros, and Geoffrey E Hinton. Layer normalization. *arXiv preprint arXiv:1607.06450*, 2016. (Cited on p. 5)
- [6] Yoshua Bengio, Andrea Lodi, and Antoine Prouvost. Machine learning for combinatorial optimization: a methodological tour d’horizon. *European Journal of Operational Research*, 290(2):405–421, 2021. (Cited on p. 2)
- [7] Timo Berthold. Measuring the impact of primal heuristics. *Oper. Res. Lett.*, 41(6):611–614, nov 2013. (Cited on p. 7)
- [8] Rainer E Burkard, Stefan E Karisch, and Franz Rendl. QAPLIB—a quadratic assignment problem library. *Journal of Global optimization*, 10(4):391–403, 1997. (Cited on p. 2, 7)
- [9] Chris Cameron, Rex Chen, Jason Hartford, and Kevin Leyton-Brown. Predicting Propositional Satisfiability via End-to-End Learning. *Proceedings of the AAAI Conference on Artificial Intelligence*, 34(04):3324–3331, Apr. 2020. (Cited on p. 2)
- [10] Quentin Cappart, Didier Chételat, Elias Khalil, Andrea Lodi, Christopher Morris, and Petar Veličković. Combinatorial optimization and reasoning with graph neural networks. *arXiv preprint arXiv:2102.09544*, 2021. (Cited on p. 2)
- [11] Quentin Cappart, Emmanuel Goutierre, David Bergman, and Louis-Martin Rousseau. Improving optimization bounds using machine learning: Decision diagrams meet deep reinforcement learning. In *Proceedings of the AAAI Conference on Artificial Intelligence*, volume 33, pages 1443–1451, 2019. (Cited on p. 2)
- [12] Yunjin Chen and Thomas Pock. Trainable nonlinear reaction diffusion: A flexible framework for fast and effective image restoration. *IEEE Transactions on Pattern Analysis and Machine Intelligence*, 39(6):1256–1272, 2017. (Cited on p. 3)
- [13] Cplex, IBM ILOG. CPLEX Optimization Studio 12.10, 2019. (Cited on p. 1)
- [14] Jian-Ya Ding, Chao Zhang, Lei Shen, Shengyin Li, Bing Wang, Yinghui Xu, and Le Song. Accelerating primal solution findings for mixed integer programs based on solution prediction. In *Proceedings of the AAAI Conference on Artificial Intelligence*, volume 34, pages 1452–1459, 2020. (Cited on p. 2)
- [15] William Falcon and The PyTorch Lightning team. PyTorch Lightning, 3 2019. (Cited on p. 7)
- [16] Matthias Fey and Jan E. Lenssen. Fast graph representation learning with PyTorch Geometric. In *ICLR Workshop on Representation Learning on Graphs and Manifolds*, 2019. (Cited on p. 7)
- [17] FICO. FICO Xpress Optimization Suite, 2022. (Cited on p. 1)
- [18] Gerald Gamrath, Daniel Anderson, Ksenia Bestuzheva, Wei-Kun Chen, Leon Eifler, Maxime Gasse, Patrick Gemander, Ambros Gleixner, Leona Gottwald, Katrin Halbig, Gregor Hendel, Christopher Hojny, Thorsten Koch, Pierre Le Bodic, Stephen J. Maher, Frederic Matter, Matthias Miltenberger, Erik Mühmer, Benjamin Müller, Marc Pfetsch, Franziska Schlösser, Felipe Serrano, Yuji Shinano, Christine Tawfik, Stefan Vigerske, Fabian Wegscheider, Dieter Weninger, and Jakob Witzig. The SCIP Optimization Suite 7.0. Technical Report 20-10, ZIB, Takustr. 7, 14195 Berlin, 2020. (Cited on p. 1)
- [19] Maxime Gasse, Didier Chételat, Nicola Ferroni, Laurent Charlin, and Andrea Lodi. Exact combinatorial optimization with graph convolutional neural networks. *arXiv preprint arXiv:1906.01629*, 2019. (Cited on p. 2, 5)

- [20] F.A. Gers, J. Schmidhuber, and F. Cummins. Learning to forget: continual prediction with LSTM. In *1999 Ninth International Conference on Artificial Neural Networks ICANN 99. (Conf. Publ. No. 470)*, volume 2, pages 850–855 vol.2, 1999. (Cited on p. 5)
- [21] Karol Gregor and Yann LeCun. Learning fast approximations of sparse coding. In *Proceedings of the 27th International Conference on International Conference on Machine Learning, ICML'10*, page 399–406, Madison, WI, USA, 2010. Omnipress. (Cited on p. 5)
- [22] Prateek Gupta, Maxime Gasse, Elias Khalil, Pawan Mudigonda, Andrea Lodi, and Yoshua Bengio. Hybrid models for learning to branch. *Advances in neural information processing systems*, 33:18087–18097, 2020. (Cited on p. 2)
- [23] Gurobi Optimization, LLC. Gurobi Optimizer Reference Manual, 2021. (Cited on p. 1, 7, 8)
- [24] Stefan Haller, Mangal Prakash, Lisa Hutschenreiter, Tobias Pietzsch, Carsten Rother, Florian Jug, Paul Swoboda, and Bogdan Savchynskyy. A primal-dual solver for large-scale tracking-by-assignment. In *AISTATS*, 2020. (Cited on p. 2, 7)
- [25] Jared Hoberock and Nathan Bell. Thrust: A parallel template library, 2010. Version 1.7.0. (Cited on p. 7)
- [26] Zeren Huang, Kerong Wang, Furui Liu, Hui-Ling Zhen, Weinan Zhang, Mingxuan Yuan, Jianye Hao, Yong Yu, and Jun Wang. Learning to select cuts for efficient mixed-integer programming. *Pattern Recognition*, 123:108353, 2022. (Cited on p. 2)
- [27] Ariel Jaimovich, Gal Elidan, Hanah Margalit, and Nir Friedman. Towards an integrated protein–protein interaction network: A relational markov network approach. *Journal of Computational Biology*, 13(2):145–164, 2006. (Cited on p. 9)
- [28] Wenzel Jakob, Jason Rhinelander, and Dean Moldovan. pybind11 – Seamless operability between C++11 and Python, 2017. <https://github.com/pybind/pybind11>. (Cited on p. 7)
- [29] Dagmar Kainmueller, Florian Jug, Carsten Rother, and Gene Myers. Active graph matching for automatic joint segmentation and annotation of *C. elegans*. In *International Conference on Medical Image Computing and Computer-Assisted Intervention*, pages 81–88. Springer, 2014. (Cited on p. 2, 7)
- [30] Diederik P Kingma and Jimmy Ba. Adam: A method for stochastic optimization. *arXiv preprint arXiv:1412.6980*, 2014. (Cited on p. 7)
- [31] Jan-Hendrik Lange and Paul Swoboda. Efficient message passing for 0–1 ILPs with binary decision diagrams. In *International Conference on Machine Learning*, pages 6000–6010. PMLR, 2021. (Cited on p. 3, 4, 6)
- [32] Fuhui Long, Hanchuan Peng, Xiao Liu, Stuart K Kim, and Eugene Myers. A 3D digital atlas of *C. elegans* and its application to single-cell analyses. *Nature methods*, 6(9):667–672, 2009. (Cited on p. 7)
- [33] Arthur Mensch and Mathieu Blondel. Differentiable dynamic programming for structured prediction and attention. In *International Conference on Machine Learning*, pages 3462–3471. PMLR, 2018. (Cited on p. 9)
- [34] Vishal Monga, Yuelong Li, and Yonina C. Eldar. Algorithm unrolling: Interpretable, efficient deep learning for signal and image processing. *IEEE Signal Processing Magazine*, 38(2):18–44, 2021. (Cited on p. 3)
- [35] Vinod Nair, Sergey Bartunov, Felix Gimeno, Ingrid von Glehn, Pawel Lichocki, Ivan Lobov, Brendan O’Donoghue, Nicolas Sonnerat, Christian Tjandraatmadja, Pengming Wang, et al. Solving mixed integer programs using neural networks. *arXiv preprint arXiv:2012.13349*, 2020. (Cited on p. 2)
- [36] Mohammadreza Nazari, Afshin Oroojlooy, Lawrence Snyder, and Martin Takáč. Reinforcement learning for solving the vehicle routing problem. *Advances in neural information processing systems*, 31, 2018. (Cited on p. 2)
- [37] NVIDIA, Péter Vingelmann, and Frank H.P. Fitzek. CUDA, release: 11.2, 2021. (Cited on p. 7)
- [38] Adam Paszke, Sam Gross, Francisco Massa, Adam Lerer, James Bradbury, Gregory Chanan, Trevor Killeen, Zeming Lin, Natalia Gimelshein, Luca Antiga, Alban Desmaison, Andreas Kopf, Edward Yang, Zachary DeVito, Martin Raison, Alykhan Tejani, Sasank Chilamkurthy, Benoit Steiner, Lu Fang, Junjie Bai, and Soumith Chintala. PyTorch: An Imperative Style, High-Performance Deep Learning Library. In H. Wallach, H. Larochelle, A. Beygelzimer, F. d’Alché-Buc, E. Fox, and R. Garnett, editors, *Advances in Neural Information Processing Systems 32*, pages 8024–8035. Curran Associates, Inc., 2019. (Cited on p. 7)

- [39] Antoine Prouvost, Justin Dumouchelle, Lara Scavuzzo, Maxime Gasse, Didier Chételat, and Andrea Lodi. Ecole: A Gym-like Library for Machine Learning in Combinatorial Optimization Solvers. In *Learning Meets Combinatorial Algorithms at NeurIPS2020*, 2020. (Cited on p. 2, 7)
- [40] Daniel Selsam, Matthew Lamm, Benedikt Bünz, Percy Liang, Leonardo de Moura, and David L Dill. Learning a SAT solver from single-bit supervision. *arXiv preprint arXiv:1802.03685*, 2018. (Cited on p. 2)
- [41] Alexander Shekhovtsov, Christian Reinbacher, Gottfried Graber, and Thomas Pock. Solving dense image matching in real-time using discrete-continuous optimization. In *Proceedings of the 21st Computer Vision Winter Workshop (CVWW)*, page 13, 2016. (Cited on p. 2)
- [42] Yunsheng Shi, Zhengjie Huang, Shikun Feng, Hui Zhong, Wenjing Wang, and Yu Sun. Masked label prediction: Unified message passing model for semi-supervised classification. In Zhi-Hua Zhou, editor, *Proceedings of the Thirtieth International Joint Conference on Artificial Intelligence, IJCAI-21*, pages 1548–1554. International Joint Conferences on Artificial Intelligence Organization, 8 2021. Main Track. (Cited on p. 5)
- [43] Nicolas Sonnerat, Pengming Wang, Ira Ktena, Sergey Bartunov, and Vinod Nair. Learning a large neighborhood search algorithm for mixed integer programs. *arXiv preprint arXiv:2107.10201*, 2021. (Cited on p. 2)
- [44] Paul Swoboda, Andrea Hornakova, Paul Roetzer, and Ahmed Abbas. Structured prediction problem archive. *arXiv preprint arXiv:2202.03574*, 2022. (Cited on p. 7)
- [45] Siddharth Tourani, Alexander Shekhovtsov, Carsten Rother, and Bogdan Savchynskyy. MPLP++: Fast, parallel dual block-coordinate ascent for dense graphical models. In *Proceedings of the European Conference on Computer Vision (ECCV)*, pages 251–267, 2018. (Cited on p. 2)
- [46] Mark Turner, Thorsten Koch, Felipe Serrano, and Michael Winkler. Adaptive cut selection in mixed-integer linear programming. *arXiv preprint arXiv:2202.10962*, 2022. (Cited on p. 2)
- [47] Jan Tönshoff, Martin Ritzert, Hinrikus Wolf, and Martin Grohe. Graph Neural Networks for Maximum Constraint Satisfaction. *Frontiers in Artificial Intelligence*, 3, 2021. (Cited on p. 2)
- [48] Vladimír Ulman, Martin Maška, Klas EG Magnusson, Olaf Ronneberger, Carsten Haubold, Nathalie Harder, Pavel Matula, Petr Matula, David Svoboda, Miroslav Radojevic, et al. An objective comparison of cell-tracking algorithms. *Nature methods*, 14(12):1141–1152, 2017. (Cited on p. 7)
- [49] Vibhav Vineet and PJ Narayanan. CUDA cuts: Fast graph cuts on the GPU. In *2008 IEEE Computer Society Conference on Computer Vision and Pattern Recognition Workshops*, pages 1–8. IEEE, 2008. (Cited on p. 2)
- [50] Tomas Werner. A linear programming approach to max-sum problem: A review. *IEEE transactions on pattern analysis and machine intelligence*, 29(7):1165–1179, 2007. (Cited on p. 4)
- [51] Thomas Windheuser, Ulrich Schlickewei, Frank R Schmidt, and Daniel Cremers. Geometrically consistent elastic matching of 3d shapes: A linear programming solution. In *2011 International Conference on Computer Vision*, pages 2134–2141. IEEE, 2011. (Cited on p. 9)
- [52] Thomas Windheuser, Ulrich Schlickewei, Frank R Schimdt, and Daniel Cremers. Large-scale integer linear programming for orientation preserving 3d shape matching. In *Computer Graphics Forum*, volume 30, pages 1471–1480. Wiley Online Library, 2011. (Cited on p. 9)
- [53] Jiadong Wu, Zhengyu He, and Bo Hong. Chapter 5 - efficient CUDA algorithms for the maximum network flow problem. In Wen mei W. Hwu, editor, *GPU Computing Gems Jade Edition*, Applications of GPU Computing Series, pages 55–66. Morgan Kaufmann, Boston, 2012. (Cited on p. 2)
- [54] Yaoxin Wu, Wen Song, Zhiguang Cao, and Jie Zhang. Learning large neighborhood search policy for integer programming. *Advances in Neural Information Processing Systems*, 34, 2021. (Cited on p. 2)
- [55] Liang Xin, Wen Song, Zhiguang Cao, and Jie Zhang. NeuroLKH: Combining Deep Learning Model with Lin-Kernighan-Helsgaun Heuristic for Solving the Traveling Salesman Problem. *Advances in Neural Information Processing Systems*, 34, 2021. (Cited on p. 2)
- [56] Zhiwei Xu, Thalaiyasingam Ajanthan, and Richard Hartley. Fast and differentiable message passing on pairwise markov random fields. In *Proceedings of the Asian Conference on Computer Vision*, 2020. (Cited on p. 2)
- [57] Yan Yang, Jian Sun, Huibin Li, and Zongben Xu. ADMM-CSNet: A Deep Learning Approach for Image Compressive Sensing. *IEEE Transactions on Pattern Analysis and Machine Intelligence*, 42(3):521–538, 2020. (Cited on p. 3)

Appendix

A Proofs

A.1 Proof of Proposition 1

The proof is an adaptation of the corresponding proof for $\omega_{ij} = 0.5$ and $\alpha_{ij} = \frac{1}{|\mathcal{J}_i|}$ given in [1].

Proof.

Feasibility of iterates. We prove

$$\sum_{j \in \mathcal{J}_i} \lambda_i^j + M_{ik} = c_i \quad (7)$$

just after line 4 and 6 in Algorithm 1. We do an inductive proof over the number of iterates w.r.t iterations t .

- $t = 0$:
- After 4: Follows from $M = 0$ in line 1.
 - After 6: Let λ', M' , be the values that are used as input to line 6 and λ and M be the ones returned in line 6. It holds that

$$\sum_{j \in \mathcal{J}_i} [\lambda_{ij} + M_{ij}] = \sum_{j \in \mathcal{J}_i} \left[\lambda'_{ij} - M_{ij}(t) + \alpha_{ij} \sum_{k \in \mathcal{J}_i} (M'_{ik}) + M_{ij} \right] \quad (8)$$

$$= \sum_{j \in \mathcal{J}_i} [\lambda'_{ij} + M'_{ij}] \quad (9)$$

$$= c_i. \quad (10)$$

by the proved inequality on λ', M' and the assumption that $\sum_{k \in \mathcal{J}_i} \alpha_{ij} = 1$.

$t > 0$: Analogously to the second point for $t = 0$.

Non-decreasing Lower Bound. In order to prove that iterates have non-decreasing lower bound we will consider an equivalent lifted representation in which proving the non-decreasing lower bound will be easier.

Lifted Representation. Introduce λ_{ij}^β for $\beta \in \{0, 1\}$ and the subproblems

$$E(\lambda_{\bullet j}^1, \lambda_{\bullet j}^0) = \min_{x \in \mathcal{X}_j} x^\top \lambda_{\bullet j}^1 + (1-x)^\top \lambda_{\bullet j}^0 \quad (11)$$

Then (D) is equivalent to

$$\max_{\lambda^1, \lambda^0} \sum_{j \in \mathcal{J}} E(\lambda_{\bullet j}^1, \lambda_{\bullet j}^0) \text{ s.t. } \sum_{j \in \mathcal{J}_i} \lambda_{ij}^\beta = \beta \cdot c_i \quad (12)$$

We have the transformation from original to lifted λ

$$\lambda \mapsto (\lambda^1 \leftarrow \lambda, \lambda^0 \leftarrow \mathbb{0}) \quad (13)$$

and from lifted to original λ (except a constant term)

$$(\lambda^1, \lambda^0) \mapsto \lambda^1 - \lambda^0. \quad (14)$$

It can be easily shown that the lower bounds are invariant under the above mappings and feasible λ for (D) are mapped to feasible ones for (12) and vice versa.

The update rule line 11 in Algorithm 1 for the lifted representation can be written as

$$\lambda_{ij}^\beta \leftarrow \lambda_{ij}^\beta - \max((2\beta - 1)M_{ij}^{out}, 0) + \alpha_{ij} \cdot \sum_{jk \in \mathcal{J}_i} \min((2\beta - 1)M_{ik}^{in}, 0) \quad (15)$$

It can be easily shown that (15) and line 11 in Algorithm 1 are corresponding to each other under the transformation from lifted to original λ .

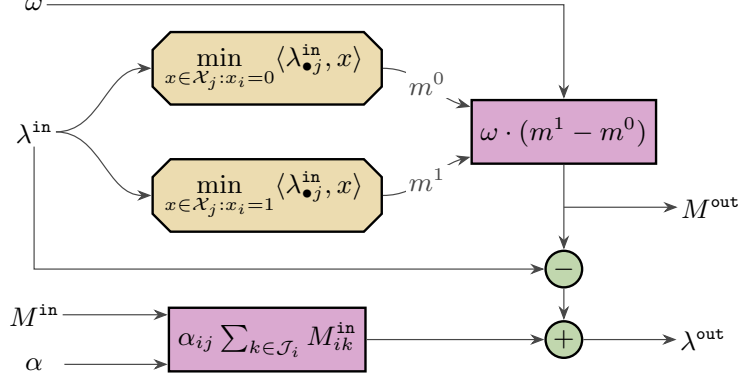


Figure 3: Computational graph of BlockUpdate in Alg. 1

Continuation of Non-decreasing Lower Bound Define

$$\lambda'_{ij} = \lambda_{ij} - \omega_{ij} \cdot \max((2\beta - 1) \left(\min_{x \in \mathcal{X}_j: x_j = \beta} \langle \lambda_{ij}^{\text{in}}, x \rangle - \min_{x \in \mathcal{X}_j: x_j = 1-\beta} \langle \lambda_{ij}^{\text{in}}, x \rangle \right), 0). \quad (16)$$

Then $E(\lambda'^{j,1}, \lambda'^{j,0}) = E(\lambda^{j,1}, \lambda^{j,0})$ are equal due to $\omega_{ij} \in [0, 1]$. Define next

$$\lambda''_{ij} = \lambda'_{ij} + \alpha_{ij} \sum_{k \in \mathcal{J}_i} \max((2\beta - 1) M_{ik}^{\text{in}}, 0). \quad (17)$$

Then $E(\lambda''^{j,1}, \lambda''^{j,0}) \geq E(\lambda'^{j,1}, \lambda'^{j,0})$ since $\lambda'' \geq \lambda'$ elementwise. This proves the claim. \square

A.2 Proof of Proposition 2

Proof. The computational graph of BlockUpdate in Alg. 1 is shown in Figure 3. Assuming gradients $\partial \mathcal{L} / \partial M^{\text{out}}$ and $\partial \mathcal{L} / \partial \lambda^{\text{out}}$ are given. We first focus on lower part of Figure 3. By applying chain rule gradient of $M_{ij}^{\text{in}} \forall ij \in B$ is computed as

$$\frac{\partial \mathcal{L}}{\partial M_{ij}^{\text{in}}} = \sum_{p \in \mathcal{I}} \sum_{k \in \mathcal{J}_p} \frac{\partial \mathcal{L}}{\partial \lambda_{pk}^{\text{out}}} \frac{\partial \lambda_{pk}^{\text{out}}}{\partial M_{ij}^{\text{in}}} = \sum_{k \in \mathcal{J}_i} \frac{\partial \mathcal{L}}{\partial \lambda_{ik}^{\text{out}}} \frac{\partial \lambda_{ik}^{\text{out}}}{\partial M_{ij}^{\text{in}}} = \sum_{k \in \mathcal{J}_i} \frac{\partial \mathcal{L}}{\partial \lambda_{ik}^{\text{out}}} \alpha_{ij}. \quad (18)$$

Similarly gradient for $\alpha_{ij} \forall ij \in B$ is

$$\frac{\partial \mathcal{L}}{\partial \alpha_{ij}} = \sum_{p \in \mathcal{I}} \sum_{k \in \mathcal{J}_p} \frac{\partial \mathcal{L}}{\partial \lambda_{pk}^{\text{out}}} \frac{\partial \lambda_{pk}^{\text{out}}}{\partial \alpha_{ij}} = \frac{\partial \mathcal{L}}{\partial \lambda_{ij}^{\text{out}}} \frac{\partial \lambda_{ij}^{\text{out}}}{\partial \alpha_{ij}} = \frac{\partial \mathcal{L}}{\partial \lambda_{ij}^{\text{out}}} \sum_{k \in \mathcal{J}_i} M_{ik}^{\text{in}}, \quad (19)$$

Since we allow running Alg. 1 for more than one iteration with same parameters (α, ω) , the above gradient (19) is accumulated to existing gradients of α to obtain the result given by Alg. 2.

For the upper part of Figure 3 we first backpropagate gradients of λ^{out} to M^{out} to account for subtraction $(-)$ as

$$\frac{\partial \mathcal{L}}{\partial M^{\text{out}}} = \frac{\partial \mathcal{L}}{\partial M^{\text{out}}} - \frac{\partial \mathcal{L}}{\partial \lambda^{\text{out}}}. \quad (20)$$

Then the gradient w.r.t. damping factors $\omega_{ij} \forall ij \in B$ is

$$\frac{\partial \mathcal{L}}{\partial \omega_{ij}} = \frac{\partial \mathcal{L}}{\partial M_{ij}^{\text{out}}} \frac{\partial M_{ij}^{\text{out}}}{\partial \omega_{ij}} = \frac{\partial \mathcal{L}}{\partial M_{ij}^{\text{out}}} (m_{ij}^1 - m_{ij}^0) = \frac{\partial \mathcal{L}}{\partial M_{ij}^{\text{out}}} \left(\frac{M_{ij}^{\text{out}}}{\omega_{ij}} \right), \quad (21)$$

which also needs to be accumulated to existing gradient as done for gradients of α .

Lastly to backpropagate gradients to λ^{in} we first calculate

$$\frac{\partial \mathcal{L}}{\partial m_{ij}^0} = \frac{\partial \mathcal{L}}{\partial M_{ij}^{\text{out}}} \frac{\partial M_{ij}^{\text{out}}}{\partial m_{ij}^0} = -\frac{\partial \mathcal{L}}{\partial M_{ij}^{\text{out}}} \omega_{ij}, \quad (22a)$$

$$\frac{\partial \mathcal{L}}{\partial m_{ij}^1} = \frac{\partial \mathcal{L}}{\partial M_{ij}^{\text{out}}} \frac{\partial M_{ij}^{\text{out}}}{\partial m_{ij}^1} = \frac{\partial \mathcal{L}}{\partial M_{ij}^{\text{out}}} \omega_{ij}. \quad (22b)$$

Then (sub-)gradient of min-marginals $m_{ij}^0, m_{ij}^1 \forall ij \in B$ w.r.t. λ^{in} are

$$\frac{\partial m_{ij}^\beta}{\partial \lambda} = \frac{\partial m_{ij}^\beta}{\partial \lambda_{\bullet j}} = \operatorname{argmin}_{x \in \mathcal{X}_j: x_{ij}=\beta} \langle \lambda_{\bullet j}, x \rangle, \quad \forall \beta \in \{0, 1\}. \quad (23)$$

Using the above relations (22), (23) and applying chain rule we obtain

$$\frac{\partial \mathcal{L}}{\partial \lambda_{ij}^{\text{in}}} = \frac{\partial \mathcal{L}}{\partial \lambda_{ij}^{\text{out}}} + \sum_{\beta \in \{0,1\}} \sum_{p \in \mathcal{I}} \sum_{k \in \mathcal{J}_p} \frac{\partial \mathcal{L}}{\partial m_{pk}^\beta} \frac{\partial m_{pk}^\beta}{\partial \lambda_{ij}^{\text{in}}} \quad (24a)$$

$$= \frac{\partial \mathcal{L}}{\partial \lambda_{ij}^{\text{out}}} + \sum_{\beta \in \{0,1\}} \sum_{p \in \mathcal{I}_j} \frac{\partial \mathcal{L}}{\partial m_{pj}^\beta} \frac{\partial m_{pj}^\beta}{\partial \lambda_{ij}^{\text{in}}}, \quad \forall ij \in B. \quad (24b)$$

□

B Efficient min-marginal computation and backpropagation

Algorithms 1 and 2 in abstract terms require solving the subproblems each time a min-marginal value (or its gradient) is required. To make these procedures more efficient we represent each subproblem as binary decision diagrams (BDD) as done in [1]. We give a short overview below and refer to [1] for more details.

Binary decision diagrams (BDD). A BDD is a directed acyclic graph with arc set A starting at a root node r and ending at two nodes \top and \perp . For each variable i the BDD contains one or more nodes in a set \mathcal{P}_i where all $r\top$ paths pass through exactly one node in \mathcal{P}_i . All $r\top$ paths in the BDD correspond to feasible assignments of its corresponding subproblem. Lagrange variables of the subproblem can be used as weights in BDD arcs allowing also to calculate cost of these $r\top$ paths. This is done by creating two outgoing arcs for a node v (except \top, \perp) in the BDD: a zero arc $vs^0(v)$ and a one arc $vs^1(v)$. If an $r\top$ path passes through zero arc $vs^0(v)$ it indicates that the corresponding variable has an assignment of 0 and 1 otherwise.

Therefore to compute the cost of assigning a 1 to variable i one needs to check all $r\top$ paths which make use of the one arcs from all nodes in \mathcal{P}_i . In [1] the authors compute min-marginals by maintaining shortest path distances. Each node v in the BDD maintains the cost of shortest path from root node r (denoted by $\text{SP}(r, v)$) and cost of shortest path to \top node. These path costs are updated in `BlockUpdate` routine of Alg. 1. Min-marginals m^0, m^1 for a variable i in subproblem j can be computed efficiently as

$$m_{ij}^\beta = \min_{\substack{vs^\beta(v) \in A \\ v \in \mathcal{P}_i}} [\text{SP}(r, v) + \beta \cdot \lambda_{ij} + \text{SP}(s^\beta(v), \top)]. \quad (25)$$

Backpropagation through min-marginals m^0, m^1 can then be done by finding the argmin in (25) instead of the min operation. Afterwards the gradients can be passed to Lagrange variables λ and shortest path costs $\text{SP}(r, \cdot), \text{SP}(\cdot, \top)$ which minimize (25). Since shortest path costs are also computed by min operations (see Alg. 3, 4 in [1]), gradients of these path costs can subsequently be backpropagated to the Lagrange variables by the argmin operation.

C Neural network details

C.1 Hand-crafted features

The features used as input to the neural networks at every optimization round are provided in Table 4.

D Results

D.1 Results on smaller instances of *QAPLib*

In Figure 4 we provide additional convergence plot calculated only on smaller instances of *QAPLib* dataset. These instances contain on average 1.6 million dual variables (instead of the overall test

Table 4: Features used for learning. Exponentially averaged features are computed with a smoothing factor of 0.9. Features corresponding to the ILP remain fixed (i.e. node degrees, constraint type, c , A , b) whereas the remaining features are updated after every optimization round.

Types	Feature description
Primal variables $f_{\mathcal{I}}$	Normalized cost vector $c/\ c\ _{\infty}$ Node degree ($ \mathcal{I}_i \forall i \in \mathcal{I}$)
Subproblems $f_{\mathcal{J}}$	Node degree ($ \mathcal{I}_j \forall j \in \mathcal{J}$) RHS vector b in constraints $Ax \leq b$ Indicator for constraint type (\leq or $=$) Current objective value per subproblem $[E^1(\bullet_j), \dots, E^m(\lambda_{\bullet_j})]$ Exp. moving avg. of first, second order change in obj. value Change in objective value due to last non-parametric update (2)
Dual variables $f_{\mathcal{E}}$	Current optimal assignment of each subproblem Exp. moving avg. of optimal assignment Coefficients of constraint matrix A Current (normalized) Lagrange variables $\lambda/\ \lambda + M + \epsilon\ $ Current (normalized) deferred min-marginal differences $M/\ \lambda + M + \epsilon\ $

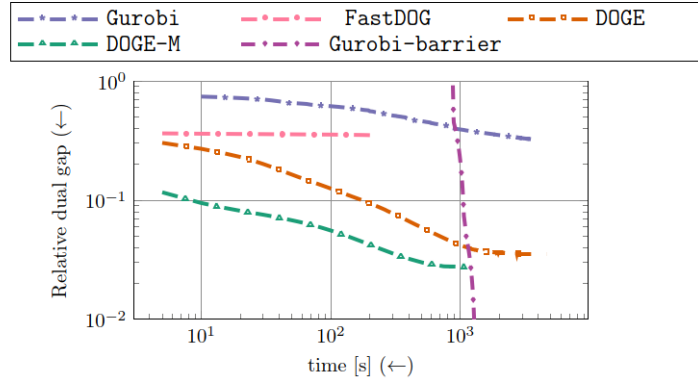


Figure 4: Convergence plots of smaller test instances of *QAPLib* (≤ 40 nodes).

split with 11 million). We observe that on relatively smaller instances our solvers DOGE, DOGE-M are surpassed by barrier method but not by dual simplex method of Gurobi. However, on larger instances barrier method could not perform any iteration within 1 hour timelimit.

D.2 Cell tracking

Table 5: Detailed results on *Cell tracking* dataset. Until termination criteria contain results where we stop our solvers early w.r.t. relative improvement. These results are averaged and reported in Table 3. Best until max. itr.: We run our solver for at most 50000 iterations and report best results (so $R = 500$, $T = 100$).

instance	method	Until termination criteria				Best until max. num itr.			
		E (\uparrow)	$g(t)$ (\downarrow)	t (\downarrow)	# itr.	E (\uparrow)	$g(t)$ (\downarrow)	t (\downarrow)	# itr.
flying-245	Gurobi	-	-	-	-	-385235600	0	809	-
	DOGE	-385424704	0.00108	1380	50000	-385424704	0.00108	1380	50000
	DOGE-M	-385428640	0.00111	730	28900	-385428544	0.00111	760	30100

D.3 Graph matching

Table 6: Detailed results on *Graph matching* dataset. Until termination criteria contain results where we stop our solvers early w.r.t. relative improvement. These results are averaged and reported in Table 3. Best until max. itr.: We run our solver for at most 10000 iterations and report best results (so $R = 50, T = 200$).

instance	method	Until termination criteria				Best until max. num itr.			
		E (\uparrow)	$g(t)$ (\downarrow)	t (\downarrow)	# itr.	E (\uparrow)	$g(t)$ (\downarrow)	t (\downarrow)	# itr.
worm10-16-03-11-1745	Gurobi	-	-	-	-	-42557	0	2356	-
	DOGE	-42645	0.00305	35	5200	-42631	0.0026	65	9600
	DOGE-M	-42611	0.00188	37.5	5600	-42599	0.00148	60	8800
worm11-16-03-11-1745	Gurobi	-	-	-	-	-48672	0	220	-
	DOGE	-48677	0.00015	12.5	3000	-48675	0.0001	25	5800
	DOGE-M	-48674	0.00006	27.5	6400	-48674	0.00005	42.5	9800
worm12-16-03-11-1745	Gurobi	-	-	-	-	-50411	0	68	-
	DOGE	-50411	0	22.5	4800	-50411	0	22.5	4800
	DOGE-M	-50411	0	25	5400	-50411	0	25	5400
worm13-16-03-11-1745	Gurobi	-	-	-	-	-45836	0	265	-
	DOGE	-45837	0.00003	15	3800	-45837	0.00003	15	3800
	DOGE-M	-45836	0	17.5	4600	-45836	0	27.5	7200
worm14-16-03-11-1745	Gurobi	-	-	-	-	-47092	0	509	-
	DOGE	-47108	0.00058	20	4400	-47100	0.00029	27.5	6000
	DOGE-M	-47100	0.00027	42.5	9400	-47100	0.00027	42.5	9400
worm15-16-03-11-1745	Gurobi	-	-	-	-	-49551	0	63	-
	DOGE	-49551	0	12.5	3200	-49551	0	12.5	3200
	DOGE-M	-49551	0	12.5	3200	-49551	0	12.5	3200
worm16-16-03-11-1745	Gurobi	-	-	-	-	-48423	0	238	-
	DOGE	-48428	0.00019	15	3800	-48427	0.00014	30	7400
	DOGE-M	-48425	0.00009	15	3800	-48424	0.00004	22.5	5600
worm17-16-03-11-1745	Gurobi	-	-	-	-	-48082	0	118	-
	DOGE	-48083	0.00001	17.5	4200	-48082	0	37.5	8800
	DOGE-M	-48083	0.00003	12.5	2800	-48082	0	20	4600
worm18-16-03-11-1745	Gurobi	-	-	-	-	-48242	0	98	-
	DOGE	-48242	0.00001	25	5200	-48242	0	32.5	6800
	DOGE-M	-48242	0	12.5	2600	-48242	0	12.5	2600
worm19-16-03-11-1745	Gurobi	-	-	-	-	-48804	0	195	-
	DOGE	-48807	0.00011	15	3400	-48806	0.00008	32.5	7200
	DOGE-M	-48806	0.00008	17.5	3800	-48805	0.00004	42.5	9400
worm20-16-03-11-1745	Gurobi	-	-	-	-	-49443	0	216	-
	DOGE	-49445	0.00009	15	3000	-49443	0.00001	42.5	8800
	DOGE-M	-49444	0.00006	37.5	7800	-49444	0.00006	37.5	7800
worm21-16-03-11-1745	Gurobi	-	-	-	-	-49844	0	67	-
	DOGE	-49844	0	20	4400	-49844	0	20	4400
	DOGE-M	-49844	0	20	4400	-49844	0	20	4400
worm22-16-03-11-1745	Gurobi	-	-	-	-	-48012	0	277	-
	DOGE	-48018	0.00022	17.5	4200	-48013	0.00002	40	9600
	DOGE-M	-48014	0.00009	20	4800	-48013	0.00003	32.5	7800
worm23-16-03-11-1745	Gurobi	-	-	-	-	-49986	0	51	-
	DOGE	-49986	0	10	2200	-49986	0	10	2200

Continued on next page

Table 6 Continued from previous page

instance	method	Until termination criteria				Best until max. num itr.			
		E (\uparrow)	$g(t)$ (\downarrow)	t (\downarrow)	# itr.	E (\uparrow)	$g(t)$ (\downarrow)	t (\downarrow)	# itr.
worm24-16-03-11-1745	DOGE-M	-49986	0	7.5	1600	-49986	0	7.5	1600
	Gurobi	-	-	-	-	-49330	0	79	-
	DOGE	-49333	0.00012	22.5	4800	-49333	0.00012	22.5	4800
	DOGE-M	-49330	0.00002	27.5	6000	-49330	0.00001	37.5	8000
worm25-16-03-11-1745	Gurobi	-	-	-	-	-47241	0	205	-
	DOGE	-47242	0.00002	17.5	4200	-47241	0	30	7200
	DOGE-M	-47242	0.00002	27.5	6600	-47241	0	37.5	9200
	Gurobi	-	-	-	-	-46145	0	595	-
worm26-16-03-11-1745	DOGE	-46161	0.00055	17.5	4000	-46158	0.00046	35	8000
	DOGE-M	-46150	0.00019	30	6800	-46148	0.00011	42.5	9600
	Gurobi	-	-	-	-	-50063	0	60	-
	DOGE	-50063	0	12.5	2600	-50063	0	12.5	2600
worm27-16-03-11-1745	DOGE-M	-50063	0	12.5	2600	-50063	0	12.5	2600
	Gurobi	-	-	-	-	-49500	0	59	-
	DOGE	-49500	0.00002	15	3400	-49500	0.00002	25	5600
	DOGE-M	-49500	0.00001	15	3200	-49500	0	27.5	6000
worm28-16-03-11-1745	Gurobi	-	-	-	-	-50070	0	46	-
	DOGE	-50070	0	15	3000	-50070	0	15	3000
	DOGE-M	-50070	0.00001	17.5	3400	-50070	0	27.5	5400
	Gurobi	-	-	-	-	-49784	0	58	-
worm29-16-03-11-1745	DOGE	-49784	0	12.5	2800	-49784	0	12.5	2800
	DOGE-M	-49784	0	15	3400	-49784	0	15	3400
	Gurobi	-	-	-	-	-50070	0	46	-
	DOGE	-50070	0	15	3000	-50070	0	15	3000
worm30-16-03-11-1745	DOGE-M	-50070	0.00001	17.5	3400	-50070	0	27.5	5400
	Gurobi	-	-	-	-	-49784	0	58	-
	DOGE	-49784	0	12.5	2800	-49784	0	12.5	2800
	DOGE-M	-49784	0	15	3400	-49784	0	15	3400

D.4 QAPLib

Table 7: Detailed results on *QAPLib* dataset. Until termination criteria contain results where we stop our solvers early w.r.t. relative improvement. These results are averaged and reported in Table 3. Best until max. itr.: We run our solver for at most 100000 iterations and report best results (so $R = 5000$, $T = 20$). *: Gurobi did not converge within 1 hour timelimit.

instance	method	Until termination criteria				Best until max. num itr.			
		E (\uparrow)	$g(t)$ (\downarrow)	t (\downarrow)	# itr.	E (\uparrow)	$g(t)$ (\downarrow)	t (\downarrow)	# itr.
bur26g*	Gurobi	-	-	-	-	9886478	0.01997	3599	-
	DOGE	10018869	0.00566	45	4820	10054780	0.00177	935	100000
	DOGE-M	10010474	0.00656	170	46340	10014676	0.00611	235	64080
bur26h*	Gurobi	-	-	-	-	6060753	0.1538	3600	-
	DOGE	7005771	0.008	50	5360	7034310	0.0036	930	99740
	DOGE-M	6997285	0.00931	185	50540	7001718	0.00863	250	68320
had20*	Gurobi	-	-	-	-	6402	0.02938	3600	-
	DOGE	6495	0.01392	280	62680	6512	0.0112	450	100000
	DOGE-M	6487	0.01532	225	99220	6487	0.01522	230	100000
kra32	Gurobi	-	-	-	-	7703	0	3333	-
	DOGE	7481	0.0317	115	12260	7545	0.02259	940	100000
	DOGE-M	7457	0.03509	360	100000	7457	0.03509	360	100000
lipa40a*	Gurobi	-	-	-	-	4217	0.91943	3597	-
	DOGE	31506	0.00109	255	5480	31538	0	2465	52920

Continued on next page

Table 7 Continued from previous page

instance	method	Until termination criteria				Best until max. num itr.			
		E (\uparrow)	$g(t)$ (\downarrow)	t (\downarrow)	# itr.	E (\uparrow)	$g(t)$ (\downarrow)	t (\downarrow)	# itr.
	DOGE-M	31417	0.00406	175	15300	31537	0.00004	1145	100000
lipa40b*	Gurobi	-	-	-	-	46637	0.92619	3598	-
	DOGE	439236	0.08045	1140	24980	442771	0.07284	1495	32760
	DOGE-M	471432	0.01109	485	43340	474399	0.0047	1120	100000
lipa50a*	Gurobi	-	-	-	-	3494	0.98823	3598	-
	DOGE	58664	0.05782	905	38720	60010	0.03512	2340	100000
	DOGE-M	61497	0.01005	145	5840	62093	0	1665	66480
lipa50b*	Gurobi	-	-	-	-	51648	0.97176	3595	-
	DOGE	1070018	0.10392	2310	99900	1070103	0.10385	2315	100000
	DOGE-M	1173647	0.01561	1190	47280	1191963	0	2490	100000
lipa60a*	Gurobi	-	-	-	-	3713	1	3595	-
	DOGE	105267	0.01789	735	15800	106426	0.00667	4660	100000
	DOGE-M	105786	0.01287	315	6420	107114	0	4955	100000
lipa60b*	Gurobi	-	-	-	-	66471	0.98356	3596	-
	DOGE	2093148	0.15489	145	3180	2186837	0.11658	4585	100000
	DOGE-M	2328269	0.05875	520	10720	2471953	0	4860	100000
lipa70a*	Gurobi	-	-	-	-	6598	0.99197	3600	-
	DOGE	165123	0.02784	1140	13160	167966	0.01054	8625	100000
	DOGE-M	167322	0.01446	565	6000	169700	0	9495	100000
lipa70b*	Gurobi	-	-	-	-	121986	0.98152	3600	-
	DOGE	4293967	0.03577	1990	23520	4382764	0.01564	4625	55120
	DOGE-M	4230582	0.05014	1355	14620	4451768	0	9310	100000
nug27*	Gurobi	-	-	-	-	2545	0.10356	3599	-
	DOGE	2693	0.04496	425	50200	2713	0.03731	850	100000
	DOGE-M	2688	0.04713	335	100000	2688	0.04713	335	100000
nug28*	Gurobi	-	-	-	-	2446	0.04303	3599	-
	DOGE	2468	0.03344	225	23300	2486	0.02522	965	100000
	DOGE-M	2456	0.03891	360	99580	2456	0.03884	365	100000
nug30*	Gurobi	-	-	-	-	1595	0.70017	3600	-
	DOGE	4481	0.07076	760	48520	4535	0.0588	1565	100000
	DOGE-M	4630	0.03817	510	99820	4630	0.03815	515	100000
rou20*	Gurobi	-	-	-	-	586646	0.09057	3599	-
	DOGE	612538	0.04922	445	99660	612560	0.04918	450	100000
	DOGE-M	612818	0.04877	225	99760	612844	0.04873	230	100000
scr20	Gurobi	-	-	-	-	75474	0	43	-
	DOGE	75401	0.00132	45	15620	75415	0.00107	140	48680
	DOGE-M	75404	0.00126	30	16620	75415	0.00106	65	36600
sko42*	Gurobi	-	-	-	-	1599	0.8898	3599	-
	DOGE	9949	0.15128	1355	99980	9949	0.15125	1360	100000
	DOGE-M	11597	0.00557	1165	78220	11659	0	1480	100000
sko49*	Gurobi	-	-	-	-	1268	0.94759	3599	-
	DOGE	15745	0.05392	2210	99800	15747	0.05383	2215	100000
	DOGE-M	16439	0.01109	1650	70580	16619	0	2340	100000
sko56*	Gurobi	-	-	-	-	1421	0.96053	3594	-
	DOGE	22410	0.06144	125	3380	23430	0.01774	3695	100000
	DOGE-M	23254	0.02529	2020	52180	23845	0	3875	100000

Continued on next page

Table 7 Continued from previous page

instance	method	Until termination criteria				Best until max. num itr.			
		E (\uparrow)	$g(t)$ (\downarrow)	t (\downarrow)	# itr.	E (\uparrow)	$g(t)$ (\downarrow)	t (\downarrow)	# itr.
sko64*	Gurobi	-	-	-	-	1053	0.98536	3586	-
	DOGE	30410	0.0819	15	240	31798	0.03917	5915	99980
	DOGE-M	31517	0.04784	2065	33000	33071	0	6255	100000
ste36c*	Gurobi	-	-	-	-	2661689	0.65051	3599	-
	DOGE	6759633	0.0412	820	26300	6967435	0.0103	3110	99660
	DOGE-M	6933566	0.01533	485	60140	6976984	0.00888	765	94840
tai35a*	Gurobi	-	-	-	-	180704	0.91506	3598	-
	DOGE	1794138	0.09976	1285	46320	1802223	0.09568	1405	50640
	DOGE-M	1896341	0.04812	735	99900	1896382	0.0481	740	100000
tai35b*	Gurobi	-	-	-	-	5212148	0.9588	3601	-
	DOGE	96397776	0.07721	540	19280	99942776	0.04294	2795	99880
	DOGE-M	98365992	0.05818	750	100000	98365992	0.05818	750	100000
tai40a*	Gurobi	-	-	-	-	121132	0.95377	3599	-
	DOGE	2140900	0.07833	480	42920	2142402	0.07768	595	53280
	DOGE-M	2321628	0	1165	100000	2321628	0	1165	100000
tai40b*	Gurobi	-	-	-	-	5241527	0.97122	3599	-
	DOGE	121210376	0.09553	295	25960	121210376	0.09553	295	25960
	DOGE-M	133862088	0	1185	100000	133862088	0	1185	100000
tai50a*	Gurobi	-	-	-	-	61532	0.98721	3592	-
	DOGE	2988845	0.18113	535	23040	2994846	0.17948	1610	69440
	DOGE-M	3622177	0.00673	2125	87480	3646619	0	2435	100000
tai50b*	Gurobi	-	-	-	-	179580	1	3599	-
	DOGE	83312440	0.1107	1995	84120	85635848	0.08563	2375	100000
	DOGE-M	93571496	0	2480	100000	93571496	0	2480	100000
tai60a*	Gurobi	-	-	-	-	87106	0.98697	3593	-
	DOGE	3984766	0.26193	265	5620	4319060	0.19975	4625	100000
	DOGE-M	5216043	0.03289	1840	38040	5392868	0	4860	100000
tai60b*	Gurobi	-	-	-	-	125579	1	3590	-
	DOGE	55250419	0.60577	255	5520	88722336	0.36445	4625	99960
	DOGE-M	106619936	0.23542	915	18680	139274272	0	4910	100000
tai64c	Gurobi	-	-	-	-	487500	0	3283	-
	DOGE	482685	0.01197	5	800	487483	0.00004	275	43760
	DOGE-M	486733	0.00191	25	760	486733	0.00191	25	760
tho30*	Gurobi	-	-	-	-	33467	0.70179	3598	-
	DOGE	90078	0.11192	945	60560	91072	0.10157	1560	100000
	DOGE-M	95420	0.05626	510	100000	95420	0.05626	510	100000
wil50*	Gurobi	-	-	-	-	3037	0.94051	3597	-
	DOGE	35943	0.08066	1655	24640	36941	0.05458	6715	100000
	DOGE-M	38775	0.00667	2140	85100	39030	0	2515	100000

D.5 Independent set

Table 8: Detailed results on *Independent set* dataset. Until termination criteria contain results where we stop our solvers early w.r.t. relative improvement. These results are averaged and reported in Table 3. Best until max. itr.: We run our solver for at most 10000 iterations and report best results (so $R = 200, T = 50$).

instance	method	Until termination criteria				Best until max. num itr.			
		E (\uparrow)	$g(t)$ (\downarrow)	t (\downarrow)	# itr.	E (\uparrow)	$g(t)$ (\downarrow)	t (\downarrow)	# itr.
1	Gurobi	-	-	-	-	-24444	0	50	-
	DOGE	-24447	0.0057	4.2	1550	-24445	0.00243	10.1	3800
	DOGE-M	-24445	0.00244	2.3	850	-24444	0.00152	3.5	1300
10	Gurobi	-	-	-	-	-24457	0	47	-
	DOGE	-24465	0.01482	4	1450	-24459	0.00427	7.3	2650
	DOGE-M	-24476	0.03372	1	350	-24459	0.00433	2.2	800
11	Gurobi	-	-	-	-	-24464	0	48	-
	DOGE	-24468	0.0075	4.2	1550	-24465	0.00276	11.1	4100
	DOGE-M	-24465	0.0032	3.2	1200	-24465	0.0023	4.4	1650
12	Gurobi	-	-	-	-	-24453	0	56	-
	DOGE	-24460	0.01384	2.7	1000	-24454	0.00268	14	5200
	DOGE-M	-24476	0.04099	1.1	400	-24454	0.00237	9.5	3350
13	Gurobi	-	-	-	-	-24461	0	56	-
	DOGE	-24466	0.00895	4	1500	-24463	0.00363	11.5	4300
	DOGE-M	-24484	0.04179	1.1	400	-24462	0.00202	5.3	2000
14	Gurobi	-	-	-	-	-24455	0	53	-
	DOGE	-24461	0.0106	3.2	1150	-24456	0.00177	13.4	4900
	DOGE-M	-24458	0.00629	2.5	900	-24458	0.00494	10.3	3800
15	Gurobi	-	-	-	-	-24467	0	50	-
	DOGE	-24474	0.01292	3.3	1200	-24469	0.00293	10.8	4000
	DOGE-M	-24469	0.00397	2.6	950	-24469	0.00277	6.8	2500
16	Gurobi	-	-	-	-	-24452	0	50	-
	DOGE	-24457	0.00917	3	1100	-24454	0.00437	10.2	3750
	DOGE-M	-24453	0.00259	2.3	850	-24452	0.00102	6	2250
17	Gurobi	-	-	-	-	-24452	0	50	-
	DOGE	-24457	0.00963	4.5	1650	-24454	0.00401	14.8	5500
	DOGE-M	-24454	0.00342	2.6	950	-24453	0.00212	7.9	2900
18	Gurobi	-	-	-	-	-24473	0	45	-
	DOGE	-24487	0.02501	2.8	1000	-24476	0.00555	11.3	4050
	DOGE-M	-24475	0.00447	2.7	950	-24474	0.00248	7.7	2800
19	Gurobi	-	-	-	-	-24458	0	59	-
	DOGE	-24467	0.01653	2.6	950	-24460	0.00368	12.6	4650
	DOGE-M	-24477	0.03407	1.1	400	-24459	0.00211	3	1100
2	Gurobi	-	-	-	-	-24459	0	45	-
	DOGE	-24464	0.00978	3.5	1250	-24460	0.00331	14.4	5350
	DOGE-M	-24464	0.0102	2.3	850	-24464	0.0102	2.3	850
20	Gurobi	-	-	-	-	-24458	0	55	-
	DOGE	-24466	0.01333	2.6	950	-24460	0.00267	12.5	4650
	DOGE-M	-24460	0.00316	2.4	900	-24459	0.0026	3.7	1350
21	Gurobi	-	-	-	-	-24458	0	55	-
	DOGE	-24470	0.02143	4.8	850	-24459	0.0033	14.9	4550
	DOGE-M	-24459	0.00269	2.4	850	-24458	0.00137	3.4	1200
	Gurobi	-	-	-	-	-24460	0	64	-

Continued on next page

Table 8 Continued from previous page

instance	method	Until termination criteria				Best until max. num itr.			
		E (\uparrow)	$g(t)$ (\downarrow)	t (\downarrow)	# itr.	E (\uparrow)	$g(t)$ (\downarrow)	t (\downarrow)	# itr.
22	DOGE	-24465	0.00884	3.7	1350	-24462	0.00414	12.5	4600
	DOGE-M	-24462	0.00313	3.6	1350	-24462	0.00286	6.1	2250
23	Gurobi	-	-	-	-	-24438	0	51	-
	DOGE	-24441	0.00678	4.8	1800	-24440	0.00385	8.9	3300
	DOGE-M	-24441	0.00617	2.3	850	-24439	0.00307	11.3	4150
24	Gurobi	-	-	-	-	-24437	0	52	-
	DOGE	-24448	0.01857	2.4	850	-24439	0.00274	10.9	4000
	DOGE-M	-24455	0.03095	1.1	400	-24439	0.00296	3.7	1350
25	Gurobi	-	-	-	-	-24468	0	47	-
	DOGE	-24477	0.0178	2.7	1000	-24470	0.00371	10.8	4000
	DOGE-M	-24489	0.03955	1.1	400	-24469	0.00317	15.4	5700
26	Gurobi	-	-	-	-	-24444	0	56	-
	DOGE	-24449	0.00899	3.4	1250	-24446	0.004	10.3	3850
	DOGE-M	-24447	0.00442	1.9	700	-24446	0.00346	3.9	1450
27	Gurobi	-	-	-	-	-24466	0	53	-
	DOGE	-24472	0.0107	4.1	1500	-24469	0.00523	15	5500
	DOGE-M	-24468	0.00308	2.1	750	-24467	0.00128	4.6	1700
28	Gurobi	-	-	-	-	-24472	0	51	-
	DOGE	-24477	0.00927	4	1300	-24473	0.00352	12.2	4300
	DOGE-M	-24492	0.03674	1	350	-24473	0.00265	6	2200
29	Gurobi	-	-	-	-	-24446	0	52	-
	DOGE	-24453	0.01268	3.3	1200	-24448	0.00365	11.1	4050
	DOGE-M	-24447	0.00231	2.6	950	-24446	0.00056	4.2	1500
3	Gurobi	-	-	-	-	-24457	0	50	-
	DOGE	-24465	0.01357	3	1100	-24459	0.00273	10.6	3900
	DOGE-M	-24479	0.03901	1.4	450	-24458	0.0022	4.6	1550
30	Gurobi	-	-	-	-	-24454	0	63	-
	DOGE	-24458	0.00777	5.3	1950	-24456	0.00296	13.7	5050
	DOGE-M	-24483	0.0518	1.4	500	-24456	0.00309	10.8	3950
31	Gurobi	-	-	-	-	-24457	0	47	-
	DOGE	-24465	0.01361	3.5	1250	-24459	0.00414	10.9	3950
	DOGE-M	-24459	0.00294	3	1100	-24458	0.0019	7.2	2650
32	Gurobi	-	-	-	-	-24466	0	41	-
	DOGE	-24474	0.01457	2.9	1050	-24468	0.00311	11.2	4100
	DOGE-M	-24487	0.03785	1.3	400	-24468	0.00273	8.4	3000
4	Gurobi	-	-	-	-	-24452	0	70	-
	DOGE	-24457	0.00847	4.4	1550	-24454	0.00316	13.3	4800
	DOGE-M	-24454	0.0041	1.8	650	-24454	0.00403	2.3	850
5	Gurobi	-	-	-	-	-24474	0	49	-
	DOGE	-24482	0.01549	2.3	850	-24476	0.003	11.1	4100
	DOGE-M	-24494	0.03738	1.1	400	-24475	0.00205	4.5	1650
59	Gurobi	-	-	-	-	-24474	0	49	-
	DOGE	-24478	0.0074	4.1	1500	-24476	0.00298	9.9	3650
	DOGE-M	-24494	0.03699	1.1	400	-24475	0.00184	7.1	2600
6	Gurobi	-	-	-	-	-24468	0	52	-
	DOGE	-24472	0.00858	4.5	1500	-24469	0.00273	10.8	3850

Continued on next page

Table 8 Continued from previous page

instance	method	Until termination criteria				Best until max. num itr.			
		E (\uparrow)	$g(t)$ (\downarrow)	t (\downarrow)	# itr.	E (\uparrow)	$g(t)$ (\downarrow)	t (\downarrow)	# itr.
60	DOGE-M	-24468	0.00156	2.9	1000	-24468	0.00068	6.2	2150
	Gurobi	-	-	-	-	-24468	0	52	-
	DOGE	-24473	0.00936	3.5	1300	-24469	0.00351	10.8	4100
61	DOGE-M	-24469	0.00186	1.9	700	-24468	0.00024	3.7	1400
	Gurobi	-	-	-	-	-24470	0	49	-
	DOGE	-24474	0.00867	4	1500	-24471	0.00237	13.8	5100
62	DOGE-M	-24472	0.00363	3.1	1150	-24471	0.0029	6	2200
	Gurobi	-	-	-	-	-24456	0	48	-
	DOGE	-24471	0.02682	2.5	900	-24459	0.00569	13.5	4900
63	DOGE-M	-24461	0.00914	2.8	1000	-24459	0.00585	13	4750
	Gurobi	-	-	-	-	-24442	0	44	-
	DOGE	-24447	0.00968	3.9	1450	-24444	0.00374	11.4	4150
64	DOGE-M	-24443	0.00289	3.1	1150	-24443	0.00235	9.6	3500
	Gurobi	-	-	-	-	-24457	0	48	-
	DOGE	-24466	0.0173	3.3	1200	-24458	0.00313	11.3	4150
65	DOGE-M	-24476	0.03412	1.1	400	-24459	0.00416	2.9	1050
	Gurobi	-	-	-	-	-24464	0	48	-
	DOGE	-24468	0.00831	4.5	1650	-24465	0.00299	10.9	4050
66	DOGE-M	-24489	0.04566	1	350	-24465	0.00211	8.1	3000
	Gurobi	-	-	-	-	-24453	0	55	-
	DOGE	-24456	0.00653	4.3	1600	-24454	0.00247	10.9	4050
67	DOGE-M	-24455	0.00379	3.5	1300	-24454	0.00223	5.4	2000
	Gurobi	-	-	-	-	-24461	0	56	-
	DOGE	-24469	0.01437	2.8	1050	-24462	0.00308	14	5250
68	DOGE-M	-24484	0.042	1.1	400	-24462	0.00176	6.3	2350
	Gurobi	-	-	-	-	-24455	0	54	-
	DOGE	-24461	0.011	3	1100	-24456	0.00235	13.2	4900
69	DOGE-M	-24458	0.00509	2.5	900	-24458	0.00506	3.1	1150
	Gurobi	-	-	-	-	-24467	0	51	-
	DOGE	-24477	0.01798	1.9	700	-24468	0.00145	8.8	3250
70	DOGE-M	-24487	0.03673	1.1	400	-24468	0.002	4.2	1550
	Gurobi	-	-	-	-	-24470	0	51	-
	DOGE	-24476	0.01197	3.1	1150	-24471	0.00282	11.8	4400
71	DOGE-M	-24489	0.03455	1.3	450	-24471	0.00269	8.1	3000
	Gurobi	-	-	-	-	-24452	0	50	-
	DOGE	-24459	0.0137	2.6	950	-24454	0.0041	11.4	4200
72	DOGE-M	-24469	0.03031	1.1	400	-24452	0.00104	7.6	2800
	Gurobi	-	-	-	-	-24452	0	48	-
	DOGE	-24464	0.02105	2.2	800	-24453	0.0023	10.5	3900
73	DOGE-M	-24468	0.028	1.5	550	-24454	0.00272	8.4	3100
	Gurobi	-	-	-	-	-24473	0	45	-
	DOGE	-24480	0.01316	3.7	1300	-24477	0.00642	9.4	3350
74	DOGE-M	-24496	0.04223	1	350	-24474	0.00207	5.3	1900
	Gurobi	-	-	-	-	-24458	0	57	-
	DOGE	-24463	0.00993	3.3	1200	-24460	0.00384	10.2	3750
75	DOGE-M	-24476	0.03355	1.1	400	-24458	0.00158	5.1	1900

Continued on next page

Table 8 Continued from previous page

instance	method	Until termination criteria				Best until max. num itr.			
		E (\uparrow)	$g(t)$ (\downarrow)	t (\downarrow)	# itr.	E (\uparrow)	$g(t)$ (\downarrow)	t (\downarrow)	# itr.
74	Gurobi	-	-	-	-	-24458	0	55	-
	DOGE	-24466	0.01417	2.3	850	-24460	0.00264	12.2	4550
	DOGE-M	-24459	0.00177	2.5	900	-24459	0.00172	5.5	1950
75	Gurobi	-	-	-	-	-24458	0	55	-
	DOGE	-24464	0.01114	3.7	1350	-24460	0.00404	9.5	3450
	DOGE-M	-24460	0.00437	2	650	-24459	0.00226	3.7	1250
76	Gurobi	-	-	-	-	-24460	0	63	-
	DOGE	-24465	0.00857	3.7	1350	-24462	0.0039	8.3	3050
	DOGE-M	-24462	0.0036	3.3	1200	-24461	0.00224	6	2200
77	Gurobi	-	-	-	-	-24438	0	48	-
	DOGE	-24443	0.00943	3.5	1300	-24440	0.00379	13	4850
	DOGE-M	-24440	0.00411	3	1100	-24439	0.00293	9.4	3450
78	Gurobi	-	-	-	-	-24437	0	52	-
	DOGE	-24446	0.01493	3.4	1250	-24440	0.00467	14.2	5250
	DOGE-M	-24439	0.00286	2.7	1000	-24438	0.00236	4.8	1800
79	Gurobi	-	-	-	-	-24468	0	46	-
	DOGE	-24477	0.01686	3.1	1150	-24470	0.00453	11.9	4400
	DOGE-M	-24490	0.04014	1.1	400	-24469	0.00282	9.8	3600
8	Gurobi	-	-	-	-	-24456	0	48	-
	DOGE	-24472	0.02816	2.3	800	-24459	0.00491	15.1	5450
	DOGE-M	-24460	0.00756	2.9	1050	-24459	0.0055	14.9	5450
80	Gurobi	-	-	-	-	-24444	0	56	-
	DOGE	-24449	0.00827	3.9	1450	-24446	0.0042	11.2	4200
	DOGE-M	-24460	0.02826	1.1	400	-24446	0.00328	2.9	1100
81	Gurobi	-	-	-	-	-24466	0	53	-
	DOGE	-24475	0.01564	2.6	950	-24468	0.00401	13.6	4950
	DOGE-M	-24467	0.00184	2.9	1050	-24467	0.001	4.3	1550
82	Gurobi	-	-	-	-	-24472	0	51	-
	DOGE	-24481	0.01659	2.2	800	-24473	0.00265	12.3	4550
	DOGE-M	-24474	0.00374	2	700	-24473	0.00264	3.9	1450
83	Gurobi	-	-	-	-	-24446	0	52	-
	DOGE	-24452	0.01118	3.7	1350	-24447	0.00281	11.8	4300
	DOGE-M	-24446	0.00169	2.8	900	-24446	0.00088	4.4	1450
84	Gurobi	-	-	-	-	-24454	0	63	-
	DOGE	-24460	0.01068	4.1	1500	-24456	0.00339	11.2	4100
	DOGE-M	-24483	0.0518	1.4	500	-24456	0.00334	11.1	3850
85	Gurobi	-	-	-	-	-24457	0	48	-
	DOGE	-24469	0.02107	3.2	1150	-24460	0.0051	10.4	3750
	DOGE-M	-24459	0.00392	2.5	900	-24458	0.00185	5.9	2150
86	Gurobi	-	-	-	-	-24466	0	41	-
	DOGE	-24476	0.01829	3.3	1200	-24469	0.00534	9.5	3500
	DOGE-M	-24468	0.00361	3.2	1150	-24468	0.00281	4.4	1600
9	Gurobi	-	-	-	-	-24442	0	44	-
	DOGE	-24448	0.01164	3.4	1200	-24443	0.0029	10.6	3850
	DOGE-M	-24443	0.00229	3.3	1200	-24442	0.00152	3.8	1350